Parametrizations of coupled betatron motion for strongly coupled lattices

Jinst

Published by IOP Publishing for Sissa Medialab

Received: *May 24, 2023*
Revised: *September 28, 2023*
Accepted: *September 29, 2023*
Published: *October 12, 2023*

Parametrizations of coupled betatron motion for strongly coupled lattices

Marion Vanwelde,[a,*] **Cédric Hernalsteens,**[a,b] **S. Alex Bogacz,**[c] **Shinji Machida**[d] **and Nicolas Pauly**[a]

[a] *Service de Métrologie Nucléaire (CP165/84), Université libre de Bruxelles, Avenue Franklin Roosevelt 50, 1050 Brussels, Belgium*
[b] *CERN, European Organization for Nuclear Research, Esplanade des Particules 1, 1211 Meyrin, Switzerland*
[c] *Thomas Jefferson National Accelerator Facility, 12000 Jefferson Avenue, Newport News, Virginia, U.S.A.*
[d] *STFC Rutherford Appleton Laboratory, Harwell Campus, Didcot, OX11 0QX, U.K.*

E-mail: marion.vanwelde@ulb.be

Abstract: The coupling of transverse motion is a natural occurrence in particle accelerators, either in the form of a residual coupling arising from imperfections or originating by design from strong systematic coupling fields. While the first can be treated perturbatively, the latter requires a robust approach adapted to strongly coupled optics, and a parametrization of the linear optics must be performed to explore beam dynamics in such peculiar lattices. This work highlights the key physical interpretations of the main parametrization formalisms to describe linear coupled optics, along with explicit links and comparisons of these parametrizations. Concepts rarely illustrated in other works, such as forced mode flips and local coupling, are explored in detail, clarifying some anomalies that can arise in lattice functions. The analytical methods have been implemented in a reference Python package and connected with ray-tracing and integration codes to explore examples of strongly coupled lattices, which are discussed in detail to highlight the key physical interpretations of the parametrizations and characteristics of the lattices.

Keywords: Accelerator modelling and simulations (multi-particle dynamics, single-particle dynamics); Beam dynamics; Beam Optics

*Corresponding author.

https://doi.org/10.1088/1748-0221/18/10/P10012

2023 JINST 18 P10012

Contents

1 Introduction

The motion of charged particles in a particle accelerator is typically studied using the linear and uncoupled theory of betatron motion. The Courant-Snyder theory [1] allows the study of unidimensional and uncoupled motion by having an elegant parametrization whose optical parameters have a clear physical meaning. However, in many machines, coupling between the two transverse degrees of freedom is present. The coupling of the particle transverse motion has long been considered an undesirable effect. This residual coupling, if not well controlled, can cause undesirable effects such as vertical emittance increase in electron synchrotrons or impact linear and nonlinear observables such as amplitude detuning [2]. To take into account the effect of residual coupling, it is possible to start from the uncoupled theory and consider the coupling as a perturbation. This perturbation theory is no longer applicable as soon as the coupling arises from strong systematic coupling fields. In this case, the machine design contains elements that introduce coupling on purpose. In colliders, it is the case for interaction regions where large solenoidal fields and compensation elements are present. Atypical optics schemes based on strong coupling insertions have also been proposed to improve the performance of lepton and hadron colliders, such as the "Möbius accelerator" [3], planar-to-circular beam adapters for circular modes operation [4], and round beam operation for lepton storage rings [5, 6].

Recently, vertical excursion fixed field accelerators (vFFAs) [7–9] have experienced a resurgence in interest [10], with their inherent coupling by design. The detailed beam dynamics study of advanced accelerator designs such as vFFAs requires models adapted to strongly coupled optics [11, 12], and a deep understanding of the existing models is thus essential. In what follows, X is the horizontal coordinate, Y is the vertical coordinate, and Z is the longitudinal coordinate in the Cartesian frame.

2023 JINST 18 P10012

In conventional, horizontal excursion, FFAs, the nonlinear magnetic field respects a scaling condition that allows having a constant tune for all energies [13–15] and higher momentum particles move to orbits of larger radius. By contrast, vFFA fields fulfill another scaling condition:

$$B = B_0 e^{k(Y-Y_0)}, \tag{1.1}$$

where $k = (1/B)(\partial B/\partial Y)$ is the normalized field gradient, Y_0 is the reference vertical position and B_0 is the magnetic field strength at the reference position. The bending field increases exponentially in the vertical direction, leading higher energy particle orbits to have the same radius but to shift vertically. The vFFA magnetic field components at any position (X, Y, Z) can be expressed with the out-of-plane polynomial expansions given in appendix A. The three field components in the median plane — the vertical plane at $X = 0$ — are [11]:

$$B_X(0, Y, Z) = 0, \tag{1.2}$$

$$B_Y(0, Y, Z) = B_0 e^{kY} g(Z), \tag{1.3}$$

$$B_Z(0, Y, Z) = \frac{B_0}{k} e^{kY} \frac{dg}{dZ}, \tag{1.4}$$

where $g(Z)$ corresponds to the magnet fringe fields. The vFFAs thus present a non-zero longitudinal field component, which arises due to the fringe fields at the vFFA element ends. It is especially important as the magnet construction, respecting the scaling law, will induce important fringe fields. By neglecting the fringe field in the element body, the transverse field components can be expressed as multipolar expansions by rewriting the exponential in terms of its Taylor series. The first-order terms of this expansion correspond to skew quadrupolar components, as explicitly shown in appendix A.

Because of the longitudinal and skew quadrupolar field components, which are the main sources of transverse motion coupling, vFFAs feature strongly coupled optics. The longitudinal and skew quadrupolar field components are the principal focusing elements in vFFAs, as there is no normal quadrupole; both coupling fields are present simultaneously, complexifying the coupled linear optics. It is therefore necessary to study vFFA lattices with a model adapted to strongly coupled optics. The choice of a given parametrization for such machines, suitable for the design, optimization, and operation phases, is key to a thorough understanding of their peculiar beam dynamics. In this work, we explore in detail the main parametrizations commonly put forth to describe coupled optics by applying them to strongly coupled lattices, such as snake [16] and spin rotator designs [17, 18]. Highlighting the interpretation, possible anomalies, and specificities of these parametrization methods is the main motivation of the present work in order to be able to apply them to vFFA designs in future studies.

Several parametrizations propose to describe coupled optics as elegantly as the Courant-Snyder theory for uncoupled motion. The most widely known parametrizations are those of Edwards and Teng (ET) [19] and of Mais and Ripken (MR) [20]. In addition, these parametrizations were extended and revisited in several works: Sagan and Rubin [21], Parzen [22], Luo [23], Wolski [24–26] and Lebedev and Bogacz (LB) [27]. The exact formalisms and notations used by these authors differ, and slightly different parametrization choices lead to an apparently inhomogeneous theory. To clarify the situation, we provide interpretations of these parameters and explicit links between them for

2023 JINST 18 P10012

the different parametrizations. While both parametrization categories can often be computed and interpreted without problems, anomalies can arise in the ET optical functions for strongly coupled lattices, resulting in potentially infinite or negative β-functions with difficult interpretation. This work illustrates this phenomenon on a Snake lattice [17], highlighting when these lattice functions diverge and can no longer be associated with finite beam sizes.

The structure of the paper is as follows. Section 2 defines specific notations that are used throughout the paper. Section 3 briefly reviews the coupling parametrizations from ET and MR, with their extensions. Physical interpretations regarding lattice functions and clarifications of the relationships between the quantities appearing in the different parametrizations are provided. The methods are implemented in the Zgoubidoo Python interface [28] for the Zgoubi code [29] and discussed in section 4 where applications are presented for example lattices and for realistic examples of snakes and spin rotators. Concepts rarely thoroughly illustrated in previous parametrization studies, such as the forced mode flip and local coupling concepts, are explored in detail, emphasizing the comparative advantages of the different parametrization formalisms. The implementations have been validated by comparing the generalized lattice functions computed by Zgoubidoo with those obtained by MAD-X [30] and PTC [31]. Conclusions and recommendations for the study of vFFA lattices are provided in section 5.

2 Notations

Lowercase bold letters are used to indicate vectors of geometric coordinates $\mathbf{x} \equiv (x\ x'\ y\ y')^T$. The vectors of canonical coordinates are designated with a hat as $\hat{\mathbf{x}} \equiv \left(x\ p_x\ y\ p_y\right)^T$. Bold uppercase letters indicate matrices (for example, $\mathbf{M}$ denotes a transfer matrix), and a hat is added when it comes to the transfer matrice over a full period ("one-turn transfer matrices" $\hat{\mathbf{M}}$). The horizontal (x) and vertical (y) directions are referred to as "physical directions" or "physical space" as opposed to the "eigen-directions" related to the directions of the decoupled motion.

To study the particle transverse motion, we use the natural coordinates of the particle that are the coordinates in the moving Frenet-Serret frame (x, y, s) attached to a reference trajectory; x and y correspond to the horizontal and vertical deviations of the particle from the reference trajectory, and the longitudinal coordinate s corresponds to the path length along this reference. In the following, we assume that the transverse components A_x and A_y of the vector potential can be written:

$$\frac{e}{p_0}A_x = -\frac{1}{2}R_1(s)y + O(y^3), \tag{2.1}$$

$$\frac{e}{p_0}A_y = \frac{1}{2}R_2(s)x + O(x^3), \tag{2.2}$$

where R_1 and R_2 are related to the longitudinal field component. In the Frenet-Serret frame, the relation between geometric coordinates and canonical variables reads:

$$x' = \frac{P_x}{p_0} - \frac{e}{p_0}A_x = \frac{P_x}{p_0} + \frac{1}{2}R_1 y, \tag{2.3}$$

$$y' = \frac{P_y}{p_0} - \frac{e}{p_0}A_y = \frac{P_y}{p_0} - \frac{1}{2}R_2 x, \tag{2.4}$$

where p_0 is the total reference momentum.

2023 JINST 18 P10012

In the matrix formalism, the solution of the equations of motion can be written in the form $\hat{\mathbf{x}}(s) = \mathbf{M}_{\mathbf{s_0 \to s}}\hat{\mathbf{x}}(s_0)$, where

$$\mathbf{M}_{\mathbf{s_0 \to s}} = \begin{pmatrix} \mathbf{A} & \mathbf{B} \\ \mathbf{C} & \mathbf{D} \end{pmatrix} \tag{2.5}$$

is the transfer matrix that propagates the physical coordinates (x, p_x, y, p_y) from s_0 to s. In the case of linear motion, the transfer matrix $\mathbf{M}_{\mathbf{s_i \to s_j}}$ is symplectic [32]:

$$\mathbf{M}^T\mathbf{S}\mathbf{M} = \mathbf{S}, \text{ where } \mathbf{S} = \begin{pmatrix} 0 & 1 & 0 & 0 \\ -1 & 0 & 0 & 0 \\ 0 & 0 & 0 & 1 \\ 0 & 0 & -1 & 0 \end{pmatrix}. \tag{2.6}$$

This symplecticity condition results in $(n^2 - n)/2$ scalar conditions. The $n \times n$ transfer matrix $\mathbf{M}$ therefore contains $\frac{n}{2}(n + 1)$ independent elements [1, 19, 27, 32]. For a two-dimensional motion, at least 10 independent parameters are needed to parameterize the matrix.

3 Comparison of transverse coupled motion parametrizations

In the case of uncoupled motion, the lattice functions $\beta(s)$, $\alpha(s)$, and $\mu(s)$ have a clear physical meaning and give information about the focusing properties of the lattice: $\beta(s)$ limits the betatron oscillation amplitude of the particles and is related to the beam size, while $\mu(s)$ represents the phase advance of the oscillation. The functions $\alpha(s)$ and $\gamma(s)$ are directly related to the β-function, while the linear tune of the periodic cell is directly related to the phase advance on a period: $Q = (\mu/2\pi)$.

Several parametrizations propose to describe the coupled optics and characterize the coupling in an elegant fashion. Among these parametrizations, the most widely known are the parametrization from Edwards and Teng [19] ("ET" parametrization) and the parametrization from Mais and Ripken [20] ("MR" parametrization). Both parametrization categories (ET and MR) provide complementary information and are generally computed for different purposes. The ET lattice functions are useful to compute the linear invariants and study the motion in the linearly decoupled planes, while the MR lattice functions can be easily linked to measurable beam parameters, such as beam sizes, and provide insight into the focusing properties of the lattice. Several authors have revisited and extended these two parametrizations: Sagan and Rubin [21], Parzen [22], Luo [23], Wolski [24–26], and Lebedev and Bogacz (LB) [27]. In this section, we briefly review the main parametrization categories (ET and MR) and their variants in order to highlight the links, similarities, and fundamental differences in the lattice parameters. The different parametrizations are applied to example lattices in section 4 to further clarify their interpretations and singularities.

3.1 Edwards and Teng (ET) parametrization

The ET parametrization transforms the coupled transfer matrix into a decoupled block-diagonal matrix using a linear similarity transformation [21]:

$$\mathbf{P}_{s_0 \to s} = \widetilde{\mathbf{R}}^{-1}(s)\mathbf{M}_{s_0 \to s}\widetilde{\mathbf{R}}(s_0), \text{ with } \widetilde{\mathbf{R}} = \begin{pmatrix} \gamma\mathbf{I} & \mathcal{C} \\ -\overline{\mathcal{C}} & \gamma\mathbf{I} \end{pmatrix}, \tag{3.1}$$

2023 JINST 18 P10012

where γ is a scalar quantity representing the coupling strength, $\mathcal{C}$ is a 2×2 matrix, $\overline{\mathcal{C}}$ is its symplectic conjugate, and $\mathbf{I}$ is the unit matrix. The decoupling matrix $\widetilde{\mathbf{R}}$ allows to go from the coupled physical space to the decoupled space in which the motion along two so-called "eigen-directions" can be described independently. This matrix can also be described as a symplectic rotation [19] that gives the orientation of the normal modes compared to the axes of the physical system, by imposing $\gamma = \cos\phi$ and $\mathcal{C} = \mathcal{D}^{-1}\sin(\phi)$, where $\mathcal{D}$ is a symplectic 2×2 matrix [19]:

$$\widetilde{\mathbf{R}} = \begin{pmatrix} \mathbf{I}\cos(\phi) & \mathcal{D}^{-1}\sin(\phi) \\ -\mathcal{D}\sin(\phi) & \mathbf{I}\cos(\phi) \end{pmatrix}, \mathcal{D} = \begin{pmatrix} a & b \\ c & d \end{pmatrix}. \tag{3.2}$$

The transfer matrix in the decoupled frame $\mathbf{P}$ propagates the decoupled coordinates (u, p_u, v, p_v) from one point to another in the accelerator: $\hat{\mathbf{u}}(s_2) = \mathbf{P}\hat{\mathbf{u}}(s_1)$. The lattice functions are defined by parametrizing each block of the block-diagonal matrix $\hat{\mathbf{P}}$ as a Twiss matrix:

$$\mathbf{A_i} = \begin{pmatrix} \cos(\mu_i) + \alpha_i\sin(\mu_i) & \beta_i\sin(\mu_i) \\ -\gamma\sin(\mu_i) & \cos(\mu_i) - \alpha_i\sin(\mu_i) \end{pmatrix}, \tag{3.3}$$

where $i = 1, 2$ indicates the considered eigenmode. The lattice functions are thus connected to the eigenmodes of oscillation and not to the physical directions of the transverse plane.

As described in [21], two solutions exist for the decoupling matrix $\widetilde{\mathbf{R}}$ when $|\mathbf{B} + \bar{\mathbf{C}}| > 0$. Depending on the chosen solution, one obtains a different block-diagonal matrix $\hat{\mathbf{P}}$, and the blocks of this matrix can be associated differently with the eigenmodes; the Twiss parameters will also have different values in one case or the other [21]. In a weakly coupled lattice, the horizontal and vertical oscillations are nearly unchanged, and the oscillation eigenmodes can be associated with the horizontal and vertical motions. The decoupling matrix must be close to the unit matrix so that the eigen-axes are close to the horizontal and vertical directions. In a strongly coupled lattice, only one solution may exist at some locations of the lattice (where $|\mathbf{B} + \bar{\mathbf{C}}| < 0$), which forces the mode identification. The change in mode identification at different locations of the lattice is referred to as *mode flipping* and only occurs in elements that introduce a strong coupling between horizontal and vertical motions. In strongly coupled lattices, the Twiss parameters can thus be different depending on the chosen mode identification. The knowledge of the ET generalized Twiss parameters is not sufficient anymore to compare lattices; the identification of the eigen-axes is required as well. The sign change of $|\mathbf{B} + \bar{\mathbf{C}}|$ characterizes a forced mode flip. When the determinant of the matrix is equal to 0, only one solution remains. When a forced mode flip occurs in the lattice, $\gamma \to 0$. The lattice functions can be discontinuous at this location, with diverging β-functions. Because the β-functions can become infinite or negative, it is not possible to preserve their physical interpretation in terms of envelope functions.

The 10 independent parameters of the ET parametrization include the generalized Twiss parameters α, β, and μ for each eigenmode of oscillation, as well as four periodic functions for the decoupling matrix $\widetilde{\mathbf{R}}$. The generalized Twiss parameters characterize the oscillations in the decoupled space, while the parameters of the matrix $\widetilde{\mathbf{R}}$ describe the coupling between the two transverse motions (strength and structure [19, 32, 33]). The Twiss parameters are defined with respect to eigen-axes that no longer correspond to the physical axes. They thus no longer have their usual physical interpretation, with the β-functions that are not directly related to the beam

2023 JINST 18 P10012

size in the physical plane. The mode identification can be tedious, and β-functions can become negative or infinite if computed with the wrong mode identification when only one solution of the decoupling matrix exists, as will be illustrated in section 4. The interpretation of the parameters of the decoupling matrix is detailed in refs. [21, 34]. Notably, $\mathcal{C}$, normalized by the β-functions, characterizes the coupling strength and can be used in coupling correction algorithms [21]. The elements of $\mathcal{C}$ are associated with the ellipse formed in the physical plane $(x - y)$ when only one of the eigenmodes is excited. In addition, the parameters of the decoupling matrix (γ and $\mathcal{C}$) can be linked to the parameters of the difference coupling resonances obtained from the perturbative approach for weak coupling [35, 36]. The parameter γ provides the coupling strength and indicates if the system is close to a coupling resonance and the type of this resonance. Finally, in the ET parametrization, the linear invariants are easily expressed in terms of the eigenmode lattice functions α, β, and μ and have the same expression as the usual Courant-Snyder invariants.

3.2 Mais and Ripken (MR) parametrization

The MR parametrization consists in parameterizing the normalization matrix — the matrix that transforms the transfer matrix into its normal form (i.e. a rotation matrix): $\mathbf{N^{-1}\hat{M}N} = \mathbf{R}(\mu_1, \mu_2)$ — with lattice functions or, in an equivalent way, parameterizing the eigenvectors of the coupled transfer matrix. The resulting lattice parameters represent the effect of the two eigenmodes of oscillation on each physical transverse direction, which allows for interpreting them in relation to the physical beam sizes. Two variants are in use for the parametrization method. The first one uses the generating vectors that define the curve formed by the turn-by-turn coordinates in phase space, as for Willeke and Ripken (WR) in ref. [37]. The second one uses the normalization matrix, as for Lebedev and Bogacz (LB) in ref. [27], and Wolski in refs. [25, 26]. Both methods ultimately parameterize the eigenvectors of the one-turn transfer matrix.

WR [37] parameterize the principal and non-principal oscillations[1] with independent lattice functions. There is a set of 20 parameters that are related to each other: (β, α, γ, ϕ, and $\tilde{\phi}$) for each mode and each transverse direction. These lattice parameters are related by [37, 38]:

$$\beta_x\phi'_x + \beta_y\phi'_y + \frac{1}{2}(R_1 + R_2)\sqrt{\beta_x\beta_y}\sin(\phi_x - \phi_y) = 1, \tag{3.4}$$

$$\tilde{\phi}(s) = \phi(s) - \arctan(\frac{\beta\phi'}{\alpha}), \quad \gamma = \frac{\beta^2\phi'^2 + \alpha^2}{\beta}. \tag{3.5}$$

The projection of the 4D phase space surface on the phase space $z - z'$ ($z = x, y$) can be characterized by the superposition of two ellipses described by the lattice functions associated with the plane and the two oscillation modes, as will be illustrated in section 4 (figure 4 for example).

LB [27] parameterize the normalization matrix with 10 independent parameters (four β-functions, four α-functions, and the two phase advances μ_1 and μ_2 appearing in the rotation matrix) and three additional real functions (ν_1, ν_2 and u). The functions ν_1 and ν_2 represent the phase shift of the non-principal oscillation linked to an eigenmode with respect to the principal oscillation of the same

[1] In the following, "main" or "principal" lattice functions denote the lattice functions in the transverse direction mainly associated with the mode eigendirection in the limit of weak coupling. Nevertheless, this denomination should not make one forget that there are no "main" β-functions in the course of strong coupling, but only four β-functions corresponding to the two eigenmodes projected on the physical axes.

2023 JINST 18 P10012

eigenmode. The principal and non-principal optical functions of WR and LB are similar, except that the coupling due to the longitudinal field is directly taken into account in the α-functions of the LB parametrization, while this is not the case in the WR parametrization. Additionally, the real function u of LB combines in a single expression the non-principal lattice functions β_{xII} and β_{yI}, the non-principal phase advances ϕ_{xII} and ϕ_{yI}, and the coupling parameters R_1 and R_2 that represent the coupling due to a longitudinal field:

$$u = \beta_{yI}\phi'_{yI} + \frac{R_2}{2}\sqrt{\beta_{xI}\beta_{yI}}\sin(\nu_1) = \beta_{xII}\phi'_{xII} - \frac{R_1}{2}\sqrt{\beta_{xII}\beta_{yII}}\sin(\nu_2). \tag{3.6}$$

This real function quantifies the lattice coupling within a single parameter. If there is no coupling in the lattice, u is zero. This parameter represents the relative importance of the x and y components of an eigenvector associated with a mode. In addition, it can also be linked to the areas of the two ellipses due to a mode in the phase planes $x - x'$, $y - y'$.

The parametrization of Wolski [26] includes the main optical functions β_x, α_x, β_y, α_y, and functions reflecting the coupling ζ_x, ζ_y, $\tilde{\zeta}_x$, $\tilde{\zeta}_y$, which combine the different non-principal optical functions appearing in WR [37] and LB [27]:

$$\zeta_x = \sqrt{\beta_{1y}}e^{-i\nu_1}, \quad \tilde{\zeta}_y = -\frac{\alpha_{1y}}{\sqrt{\beta_{1y}}}e^{i\nu_1} - i\frac{u}{\sqrt{\beta_{1y}}}e^{i\nu_1}, \tag{3.7}$$

$$\zeta_y = \sqrt{\beta_{2x}}e^{-i\nu_2}, \quad \tilde{\zeta}_x = -\frac{\alpha_{2x}}{\sqrt{\beta_{2x}}}e^{i\nu_2} - i\frac{u}{\sqrt{\beta_{2x}}}e^{i\nu_2}. \tag{3.8}$$

The motion in the x-direction can be seen as the superposition of two quasi-harmonic motions. The "main" motion corresponds to the projection of the oscillation mode I in the x-direction, leading to a quasi-harmonic oscillation whose amplitude is characterized by β_x and which is in phase with the oscillation in the eigen direction I. The "non-principal" motion corresponds to the projection of the oscillation mode II in the x-direction, resulting in a quasi-harmonic oscillation whose amplitude is characterized by $|\zeta_y| = \sqrt{\beta_{2x}}$ and whose phase shift compared to the oscillation eigenmode II is $-\nu_2$.

The parameters appearing in the different parametrizations of the MR category are summarized in table 1. In addition to these approaches, which are restricted to a minimal number of parameters, it should be noted that parametrizations with more parameters have also been proposed [24]. Considering additional parameters allows having similar expressions for all the lattice functions, as well as elegant expressions for the correlation matrix elements in terms of these generalized lattice functions.

To summarize, the parameter set of the MR parametrization generally includes two main phase advances, four main lattice functions β, α, or γ, and parameters reflecting the coupling. Variants exist for the coupling parameters describing the off-diagonal part of the normalization matrix. These parameters are described either by non-principal β, α, and phase advances as in the parametrizations of WR and LB [27, 37], or by complex parameters which combine these non-principal functions into a single quantity as in the parametrization of Wolski [26]. The non-principal optical functions are characteristics of the coupling. If there is no coupling, the non-principal β and α functions (or equivalently the complex ζ functions) are zero: $\beta_{1y} = \beta_{2x} = \alpha_{1y} = \alpha_{2x} = \zeta_y = \zeta_x = u = 0$.

The physical interpretation of the MR parameters is similar to the usual Twiss interpretation of the Σ matrix of the second-order moments in the physical laboratory axes. This constitutes the main advantage of this parametrization. The β-functions (and the modulus of ζ), which are positive and finite functions (unlike the β-functions of the ET parametrization), characterize the amplitude of the

2023 JINST 18 P10012

Table 1. Comparison of the parameters appearing in [27], [37] and [26].

Principal lattice functions		
Willeke & Ripken [37]	Lebedev & Bogacz [27]	Wolski [26]
β_{xI}	β_{1x}	β_x
β_{yII}	β_{2y}	β_y
$\alpha_{xI} + \frac{R_1}{2}\sqrt{\beta_{xI}\beta_{yI}}\cos(\nu_1)$	α_{1x}	α_x
$\alpha_{yII} - \frac{R_2}{2}\sqrt{\beta_{xII}\beta_{yII}}\cos(\nu_2)$	α_{2y}	α_y
ϕ_{xI}	μ_1	μ_I
ϕ_{yII}	μ_2	μ_{II}
Non-principal lattice functions		
Willeke & Ripken [37]	Lebedev & Bogacz [27]	Wolski [26]
β_{xII}	β_{2x}	$\lvert\zeta_y\rvert^2$
β_{yI}	β_{1y}	$\lvert\zeta_x\rvert^2$
$\alpha_{xII} + \frac{R_1}{2}\sqrt{\beta_{xII}\beta_{yII}}\cos(\nu_2)$	α_{2x}	$-Re(\zeta_y\tilde{\zeta}_x)$
$\alpha_{yI} - \frac{R_2}{2}\sqrt{\beta_{xI}\beta_{yI}}\cos(\nu_1)$	α_{1y}	$-Re(\zeta_x\tilde{\zeta}_y)$
ϕ_{xII}	$\mu_1 - \nu_1$	$\mu_I + ph(\zeta_x)$
ϕ_{yI}	$\mu_2 - \nu_2$	$\mu_{II} + ph(\zeta_y)$

transverse betatron oscillations and are related to the horizontal and vertical beam sizes; they allow to easily generalize the envelope expression of the uncoupled motion. The α-functions also have the same meaning as in Courant-Snyder's theory if there is no longitudinal field that couples motion. Otherwise, the α-functions of the WR parametrization will remain identical, while the α parameters of the other parametrizations will have an additional term that accounts for this longitudinal field coupling. The MR parametrization allows computing the elements of the correlation matrix explicitly, as shown in table 2.

Table 2. Correlation matrix elements with the parameters appearing in [27] and [26].

Elements	Lebedev & Bogacz [27]	Wolski [26]
$< x^2 >$	$\beta_{1x}\varepsilon_I + \beta_{2x}\varepsilon_{II}$	$\beta_{1x}\varepsilon_I + \lvert\zeta_y\rvert^2\varepsilon_{II}$
$< y^2 >$	$\beta_{1y}\varepsilon_I + \beta_{2y}\varepsilon_{II}$	$\lvert\zeta_x\rvert^2\varepsilon_I + \beta_{2y}\varepsilon_{II}$
$< xy >$	$\sqrt{\beta_{1x}\beta_{1y}}cos(\nu_1)\varepsilon_I + \sqrt{\beta_{2x}\beta_{2y}}cos(\nu_2)\varepsilon_{II}$	$\sqrt{\beta_{1x}}Re(\zeta_x)\varepsilon_I + \sqrt{\beta_y}Re(\zeta_y)\varepsilon_{II}$
$< xp_x >$	$-\alpha_{1x}\varepsilon_I - \alpha_{2x}\varepsilon_{II}$	$-\alpha_{1x}\varepsilon_I + Re(\zeta_y\tilde{\zeta}_x)\varepsilon_{II}$
$< yp_y >$	$-\alpha_{1y}\varepsilon_I - \alpha_{2y}\varepsilon_{II}$	$Re(\zeta_x\tilde{\zeta}_y)\varepsilon_I - \alpha_{2y}\varepsilon_{II}$

The particle distribution is characterized by the mode emittances ε_1 and ε_2, which are invariants of motion in linear optics, and the 4D beam emittance is defined by the product of the mode emittances $\varepsilon_{4D} = \varepsilon_1\varepsilon_2$ [27]. The expression of the Σ matrix using the MR parameters provides a path to the beam-based measurements of these parameters. In ref. [25], Wolski presents an experimental method to obtain the phase advances and ratios of lattice functions (β-functions and ζ modulus)

2023 JINST 18 P10012

from beam position monitor (BPM) measurements. In ref. [23], Luo establishes a procedure to reconstruct the normalization matrix from turn-by-turn BPM data. In his work, the normalization matrix is written in the most general way without parametrizing the matrix elements using amplitude and phase functions. It gives insight into the practical use of the normalization matrix [35].

3.3 Relationships between ET and MR parametrizations

The ET parametrization directly expresses the linear invariants in terms of the Twiss parameters in the decoupled space, and the MR parametrization provides direct expressions for the Σ matrix in terms of the generalized Twiss parameters. Expressing the linear invariants with the MR parametrization or expressing the Σ matrix with the ET parametrization proves difficult. The link between these parametrizations was clarified by Lebedev and Bogacz in ref. [27]. They have highlighted the relations between the parameters involved in the two types of parametrizations:

$$1-u=\cos^2\phi \qquad \Rightarrow \sin\phi=\pm\sqrt{u}, \tag{3.9}$$

$$\beta_{1x}=\beta_1\cos^2\phi \qquad \Rightarrow\beta_1=\frac{\beta_{1x}}{1-u}, \qquad \beta_{2y}=\beta_2\cos^2\phi \qquad \Rightarrow\beta_2=\frac{\beta_{2y}}{1-u}, \tag{3.10}$$

$$\alpha_{1x}=\alpha_1\cos^2\phi \qquad \Rightarrow\alpha_1=\frac{\alpha_{1x}}{1-u}, \qquad \alpha_{2y}=\alpha_2\cos^2\phi \qquad \Rightarrow\alpha_2=\frac{\alpha_{2y}}{1-u}. \tag{3.11}$$

The parameter u, which reflects the coupling in the LB parametrization, is related to the rotation angle in the ET parametrization. When the parameter u is negative, the ET rotation angle ϕ is complex. It is equivalent to the situation where $|\mathbf{B}+\bar{\mathbf{C}}|<0$, meaning that only one solution exists for the ET parametrization. When the parameter u changes sign, a mode flip is forced. As mentioned by LB in ref. [27], the phase advances μ_1 and μ_2 are the same in the ET and the MR parametrizations.

The MR parametrization allows univocally determining the generalized Twiss parameters from the transfer matrix eigenvectors, with no mode identification problems. Nevertheless, it is impossible to uniquely determine the eigenvectors if only the lattice functions are given. By contrast, the knowledge of the ET generalized Twiss parameters allows uniquely determining the eigenvectors, but it is impossible to uniquely determine the ET parameters from the knowledge of these eigenvectors. Knowing the eigenvectors of the coupled transfer matrix allows for calculating the parameter u, but there are four possible ET rotation angles ϕ for a given parameter u. To determine the generalized ET Twiss parameters from the coupled transfer matrix, it is necessary to choose ϕ, or equivalently, to choose one of the possible solutions for the decoupling matrix (distinct mode identifications).

4 Applications of the parametrizations on typical and strongly coupled lattices

The ET and LB parametrizations have been implemented in Zgoubidoo [28], a Python interface for the ray-tracing code Zgoubi [29, 39, 40], and validated by comparing with the coupled lattice functions obtained with MAD-X [30] and PTC [31]. Ray-tracing codes, like Zgoubi, allow particles to be tracked in arbitrary electro-magnetic fields. The ability to perform step-by-step tracking makes Zgoubi a method of choice for (v)FFA studies [12, 41–43]. Zgoubidoo provides a user-friendly Python interface and is capable of processing the tracking data to extract relevant quantities for beam dynamics studies [44].

The ET parametrization was implemented using the method presented by Parzen [22] and allows for finding linear invariants. This method is advantageous because it allows studying the

2023 JINST 18 P10012

coupled motion in a phase space of greater dimension: for example, the ET parametrization is extended by Parzen for coupled motion in 6 degrees of freedom [22]. The LB parametrization was chosen among all the parametrizations of the MR category because it provides interesting additional quantities (u, ν_1, ν_2) together with the lattice functions of the WR parametrization. The LB lattice functions provide the evolution of the beam envelope in the laboratory axes along the lattice. The implementations were first tested on weakly coupled example lattices, then validated with more complicated strongly coupled lattices against results obtained with MAD-X for the ET parametrization [33], and MAD-X combined with PTC for the MR parametrization [30, 31]. The different parametrization methods allow, on the one hand, to find the periodic conditions for periodic lattices and, on the other hand, to propagate initial lattice functions in a beamline. The examples presented below validate both the computation of coupled periodic lattice functions and the propagation of initial lattice functions. In addition, forced mode flips, local coupling, and interpretation of lattice parameters are analyzed in detail. Table 3 summarizes the different example lattices discussed in this section, with the lattice function computation method (periodic conditions or propagation of initial lattice functions) and the concepts the example illustrates.

Table 3. Examples used to validate the parametrization implementation and illustrate some peculiar concepts and parameter interpretation. "Periodic" stands for "Periodic initial conditions", while "Propagation" stands for "Propagation of initial lattice functions".

Examples	Computation	Illustration
FODO + skew quad	Periodic	- Global coupling and u parameter - ET/MR functions to characterize decoupled and coupled phase spaces
FODO + solenoid	Periodic	- WR/LB param. (MR category) characterizing geometric and canonical coupled phase spaces
Snake lattice [17]	Propagation	- Forced mode flip - Local coupling and u parameter
Spin rotator [17]	Propagation	- Local coupling and u parameter

The longitudinal and skew quadrupolar field components being the principal coupling sources, the weakly coupled lattice examples are FODO lattices featuring short skew quadrupolar or solenoid insertions. One can observe in figures 1 and 2 that an excellent agreement is found between the lattice functions computed with Zgoubidoo (ET and LB parametrizations) and those computed with MAD-X (ET parametrization) combined with PTC (MR parametrization), for the two weakly coupled example FODO lattices. In addition, the phase advances μ_1 and μ_2 obtained from the ET and MR parametrizations are identical, as expected. It should be noted that the solenoid models in MAD-X and Zgoubi are different, which may introduce differences in the computed lattice functions. MAD-X models a hard-edge solenoid, while Zgoubi models a more realistic solenoid with fringe fields whose length depends on the solenoid (finite) radius.

When computing these lattices, the initial conditions were obtained assuming a periodic transfer matrix. The lattice functions represented in figures 1 and 2 are thus periodic optical functions and reflect the global coupling of the lattice. This global coupling can be understood by analyzing the lattice

2023 JINST 18 P10012

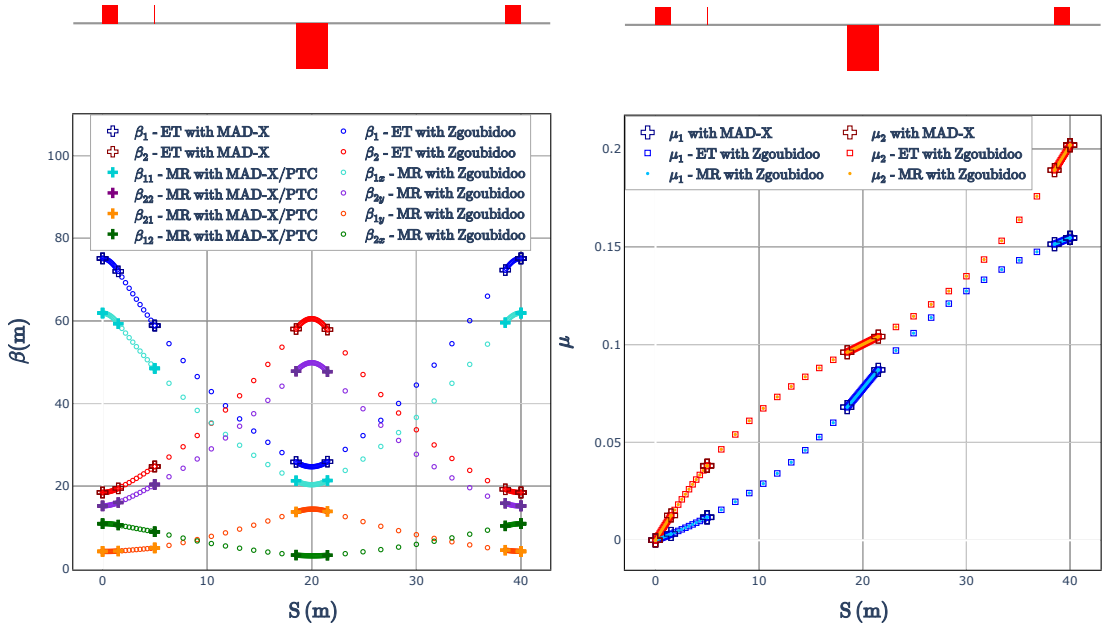

Figure 1. Comparison between the coupled lattice functions (ET and MR parametrizations) obtained with Zgoubidoo and those obtained with MAD-X and PTC on a lattice consisting of a FODO with a small skew quadrupole. The MR-category parametrization implemented in Zgoubidoo is the LB parametrization.

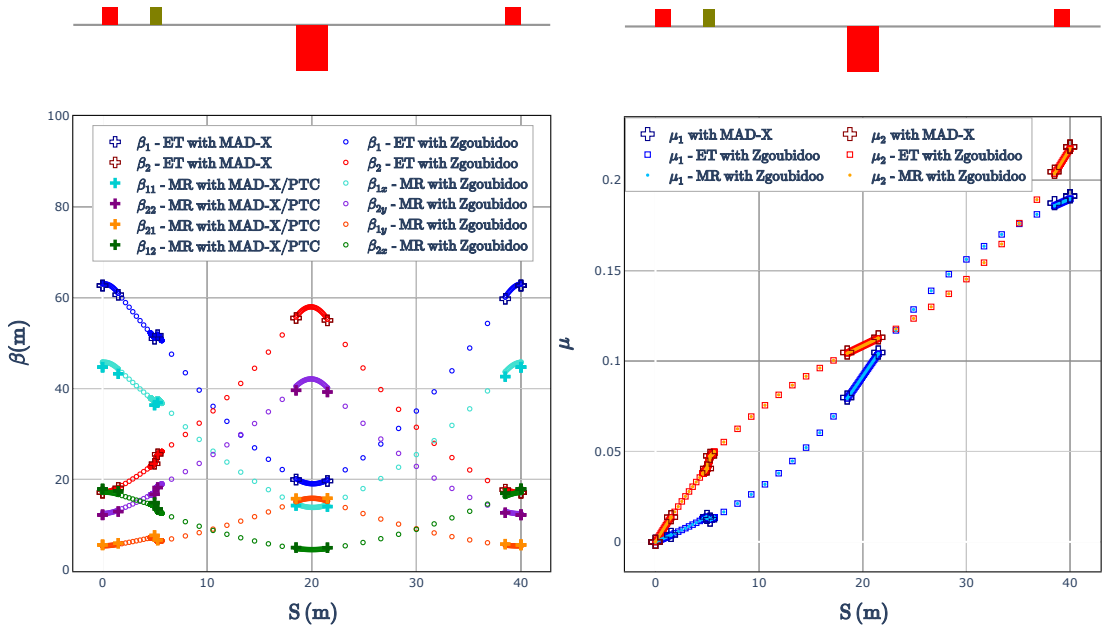

Figure 2. Comparison between the coupled lattice functions (ET and MR parametrizations) obtained with Zgoubidoo and those obtained with MAD-X and PTC on a lattice consisting of a FODO with a small solenoid. The MR-category parametrization implemented in Zgoubidoo is the LB parametrization.

parameters of LB. The non-principal lattice functions (β_{1y} and β_{2x}) are non-zero at the beginning of the lattice. They are computed with periodic conditions and therefore take into account the coupling present in the whole lattice and not only the coupling at the location where they are calculated. The

2023 JINST 18 P10012

coupling is distributed over the entire line. The LB parameter u on the full lattice remains constant on the entire line at a value of 0.176. When computed with periodic conditions, this parameter gives a measure of the overall coupling of the lattice. It provides insight into the weight of the non-principal lattice functions compared to the principal ones over the complete lattice. A fully coupled lattice would have principal functions equal to the non-principal ones and $u = 0.5$; it is the case, for example, of a FODO cell in which all the elements are rotated by 45 degrees. The parameter u has constant values in the elements not introducing coupling but varies in the elements introducing coupling and indicates whether the element couples more or less the motion than the lattice does globally.

The parameter u can also be linked to the area of the ellipses in the coupled phase spaces. Figures 3a and 3b show the decoupled phase space $(u - p_u)$ and the coupled phase space $(x - p_x)$, obtained by tracking over 1000 iterations a particle with an initial horizontal amplitude in the FODO cell with the additional skew quadrupole. We observe that the lattice functions of the ET parametrization allow describing the ellipse in the decoupled phase space, while the lattice functions of the MR parametrization allow describing the two ellipses in the coupled phase space. The area of the ellipse in the phase space $(u - p_u)$ is given by $\pi\epsilon_1$ and is an invariant of the motion, while the areas of the ellipses corresponding to the two oscillation modes projected into the transverse phase plane $(x - p_x)$ can be calculated using the parameters of LB: $\Gamma_{1x} = \pi\epsilon_1(1 - u)$, $\Gamma_{2x} = \pi\epsilon_2 u$. The parameter u gives the relative importance of the two ellipses coming from an oscillation eigenmode in the two transverse phase spaces $(x - p_x)$ and $(y - p_y)$.

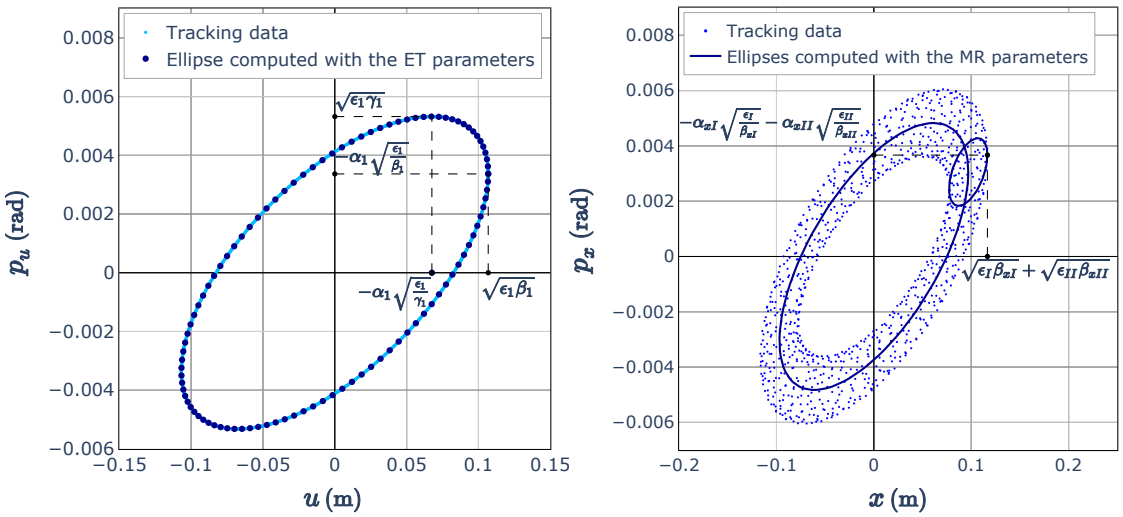

(a) (b)

Figure 3. (a) Decoupled phase space $(u - p_u)$ obtained by tracking a particle over 1000 iterations in a cell composed of a FODO with a skew quadrupole. The ET lattice functions describe the decoupled phase space ellipse whose area is $\pi\epsilon_1$. (b) Coupled phase space $(x - p_x)$ obtained by tracking a particle over 1000 iterations in a cell composed of a FODO with a skew quadrupole. The MR lattice functions characterize the two ellipses due to the two oscillation eigenmodes appearing in the coupled phase space. The ellipse areas are given by $\pi\epsilon_1(1 - u)$ and $\pi\epsilon_2 u$.

When the phase space corresponds to geometric variables $(x - x')$, the chosen MR lattice functions are those of WR rather than those of LB. Indeed, the major difference between the β

2023 JINST 18 P10012

and α-functions of WR and those of LB comes from considering or not the coupling due to the longitudinal magnetic field (see table 1). In the example of the FODO with a skew quadrupole, there is no longitudinal field at the place where the coordinates are sampled ($R_{1,2} = 0$). The lattice functions of WR and those of LB are thus equivalent, and the phase spaces in canonical or geometric coordinates are the same. In the example of the FODO with a solenoid, it is possible to sample the coordinates at a place where the longitudinal field is non-zero. The phase spaces in geometric or canonical coordinates are then very different, as shown in figure 4. The phase space portraits obtained in each case are characterized by the superposition of two ellipses. These ellipses are described by the WR parameters in the geometric case and by the LB parameters in the canonical case.

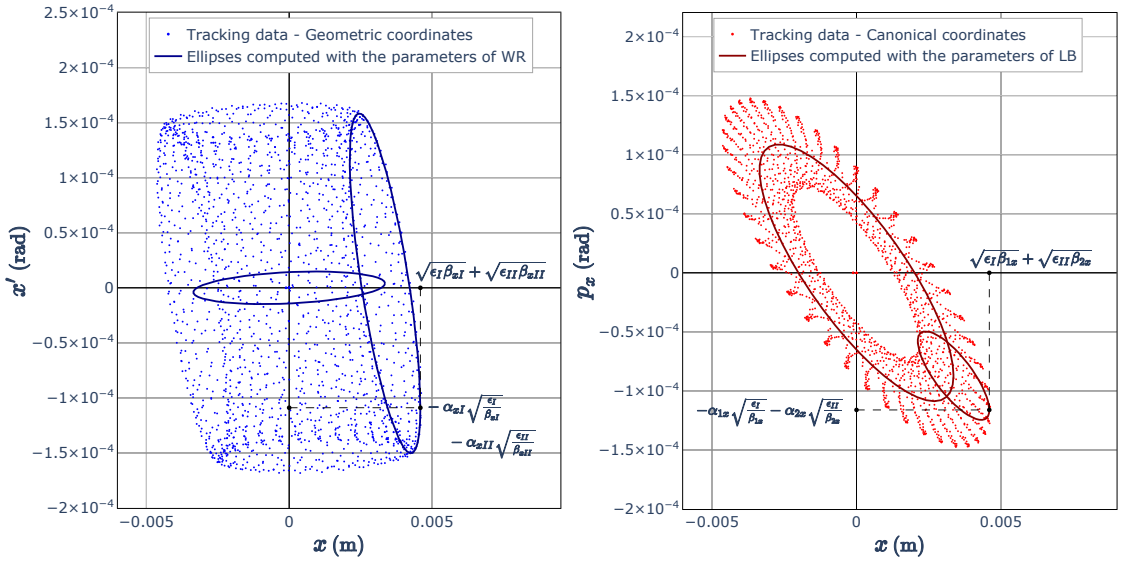

Figure 4. Coupled phase spaces in geometric (left) or canonical (right) coordinates. The lattice functions of WR describe the geometric phase space, while the lattice functions of LB describe the canonical phase space by taking into account the longitudinal field.

As examples for more complex strongly coupled lattices, we used a "Snake" lattice [16, 17], illustrated in figure 5, and a "Spin Rotator" beamline [17, 18]. The calculation of the lattice functions was done by propagating initial conditions. The initial lattice functions are not coupled, meaning

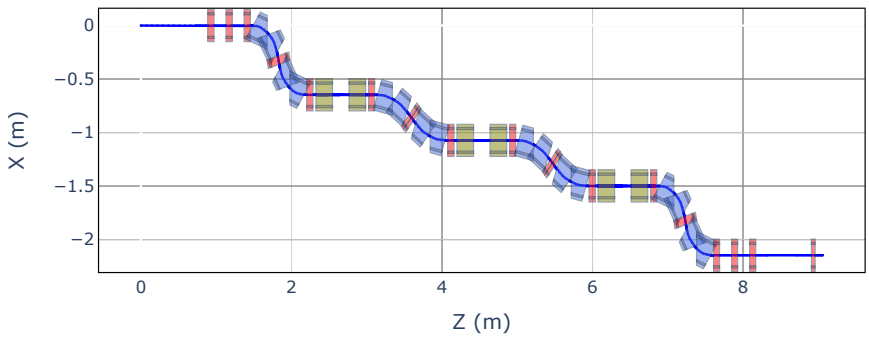

Figure 5. Representation of the example Snake lattice. Quadrupoles are depicted in red, dipoles in blue, and solenoids in yellow.

that the coupling parameters are zero: in the ET parametrization, the decoupling matrix equals the identity; in the MR parametrization, non-principal lattice functions and additional parameters (u, ν_1, ν_2) are zero at the beginning of the transfer line. Figure 6 shows the comparison of the coupled β-functions (in the ET and MR parametrizations) computed with Zgoubidoo and those obtained with MAD-X and PTC on the Snake lattice. We see a good agreement, even if there are some discrepancies due to the difference in the solenoid model. Figure 7 shows the same comparison but on the Spin Rotator lattice. Again, an excellent agreement is found.

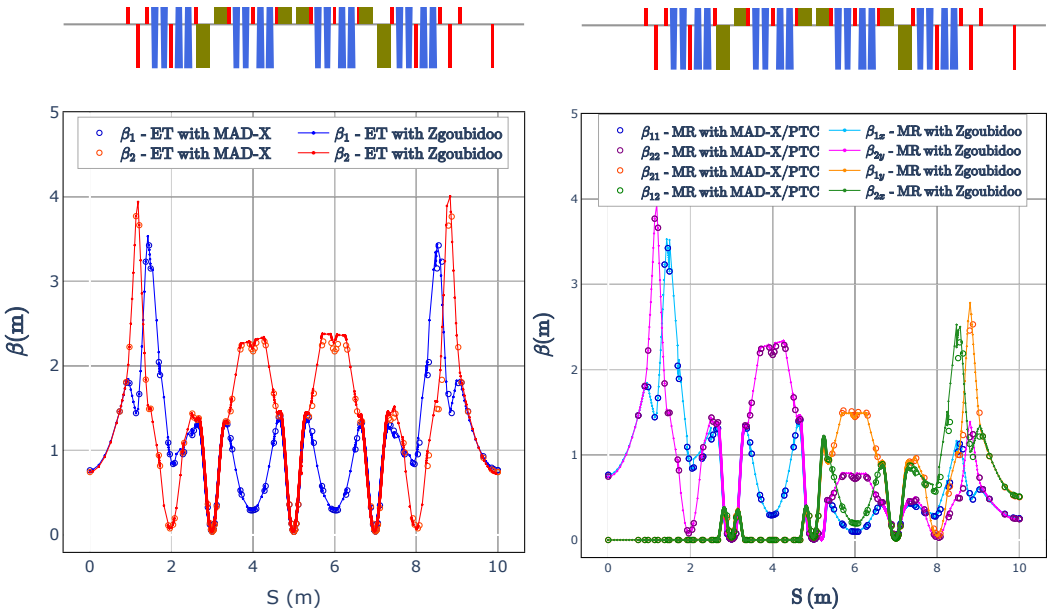

Figure 6. Comparison between the coupled β-functions (ET and MR parametrization) obtained with Zgoubidoo and those obtained with MAD-X and PTC on the Snake lattice. The MR-category parametrization implemented in Zgoubidoo is the LB parametrization. The data points obtained with Zgoubidoo are joined by interpolating straight lines to highlight the overall shape of the lattice functions.

The propagation of lattice functions allows for an in-depth study of other key concepts such as forced mode flip and local coupling concepts. In the Snake lattice, we can highlight the problems related to forced mode flips by propagating the β-functions of the ET parametrization. Figure 8a shows the evolution of the ET γ parameter throughout the lattice. By propagating initial lattice functions, a forced mode flip can occur when $\gamma \to 0$. Figure 8b shows the β-functions and γ parameter of the ET parametrization on a portion of the transfer line. When $\gamma \to 0$, the β-functions of ET seem to diverge; it illustrates that the ET lattice functions can sometimes be discontinuous or negative. Therefore, they cannot be related to the beam size.

In this example, the transfer matrix in decoupled space is block-diagonal at all lattice points, which indicates that there is no mode flip between the start and the end of the lattice. The initial mode identification is kept throughout the transfer line due to Parzen's method [22] used to implement the ET parametrization. This method solves the problem of mode identification of the ET parametrization because it is based on the eigenvectors of the transfer matrix. Each eigenvector is associated with an eigenvalue. The eigenvalues of **M** being the same as those of **P** (matrices related by a similarity transformation), the oscillation eigenmodes can also be associated with these eigenvalues. To keep

2023 JINST 18 P10012

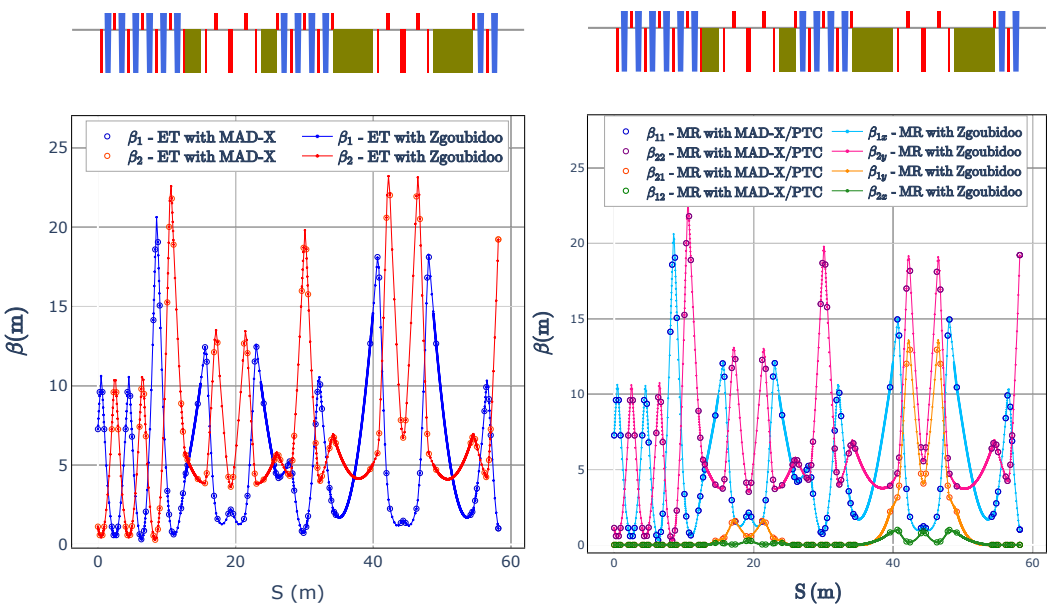

Figure 7. Comparison between the coupled β-functions (ET and MR parametrization) obtained with Zgoubidoo and those obtained with MAD-X and PTC in the Spin Rotator lattice. The MR-category parametrization implemented in Zgoubidoo is the LB parametrization. The data points obtained with Zgoubidoo are joined by interpolating straight lines to highlight the overall shape of the lattice functions.

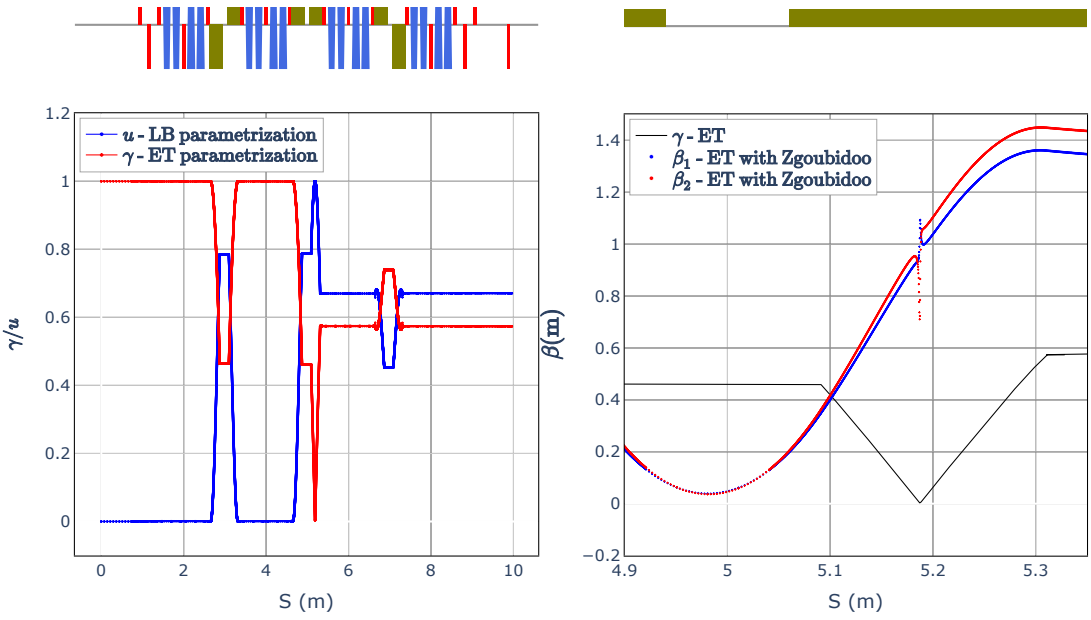

(a) (b)

Figure 8. (a) Parameter u of the LB parametrization and γ of the ET parametrization, obtained by the propagation of initial lattice functions on the Snake lattice. (b) β-functions and γ parameter of the ET parametrization on a portion of the Snake line. This figure is a zoom on the lattice location that shows forced mode flip conditions ($\gamma \to 0$). At this location, the β-functions can diverge and can not anymore be related to beam sizes.

2023 JINST 18 P10012

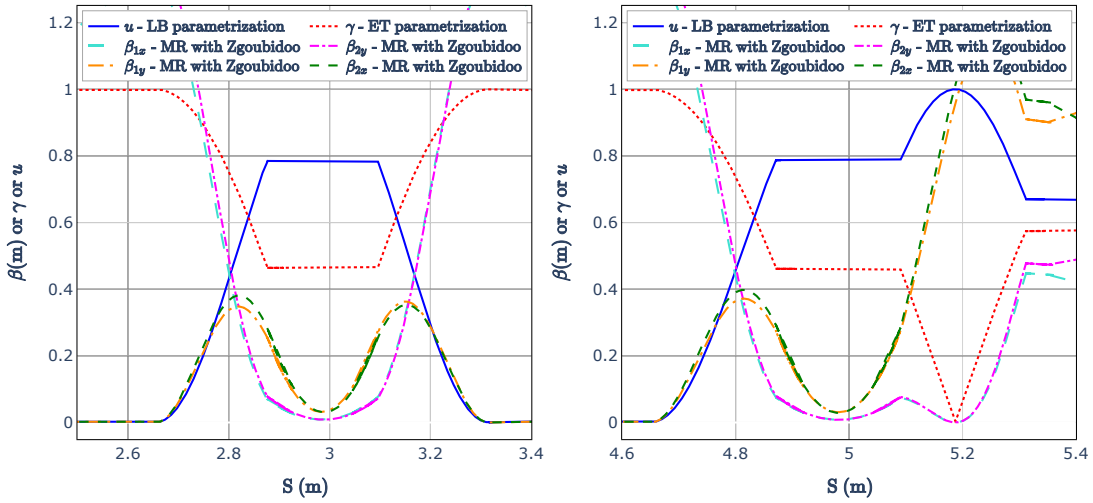

Figure 9. β-functions and u parameter of the LB parametrization in addition to the γ parameter of the ET parametrization. This figure is a zoom on lattice portions where $u > 0.5$, including the lattice location that shows forced mode flip conditions ($\gamma \to 0$). When $u > 0.5$, the non-principal functions become more important than the principal ones.

a specific mode identification throughout the lattice, it is thus sufficient to calculate the optical parameters of each eigenmode with the eigenvectors of the coupled transfer matrix corresponding to the same eigenvalues. One can thus ensure that the Twiss parameters always correspond to the same oscillation eigenmode. This method allows removing the mode flips.

However, when a mode flip is "forced", it means that the mode identification is incorrect: it is not possible to correctly compute lattice functions with this mode identification. At the location of a forced mode flip, the planes are completely exchanged. The eigen-axes correspond to the horizontal and vertical axes (x and y), but the axes are switched; the two modes are identified with the perpendicular axes so that the β-functions diverge totally. When $\gamma \to 0$, the transfer matrix in the coupled space tends towards an anti-diagonal matrix: any initial offset in x is transformed almost entirely into a motion in y and vice versa, confirming the interpretation of the total axes exchange due to the strong coupling of the lattice. To summarize, when a forced mode flip condition occurs at some place of the lattice ($\gamma \to 0$), either the mode identification is changed, which allows keeping finite β-functions but poses mode identification difficulties, or the mode identification is kept, which leads to lattice functions that can diverge and can no longer be associated with finite beam sizes.

By analyzing the β-functions of the MR parametrization (see figure 9), we note that this phenomenon results in the fact that a mode is first more reflected on a plane and then more on the other plane. When $\gamma \to 0$ ($s \approx 5.19\,\mathrm{m}$), the main β-functions (β_{1x} and β_{2y}) are zero, and the eigenmode oscillations are reflected on the other axis, which translates into non-principal lattice functions (β_{1y} and β_{2x}). Finally, it should be noted that the forced mode flip conditions in this lattice appear inside a solenoid. The potential problems are thus only fully detected when the tracking code allows step-by-step tracking inside the elements. Zgoubidoo, with Zgoubi in the backend, allows for obtaining step-by-step transfer matrices and thus detecting any potential problem related to the ET parametrization.

In addition to the forced mode flips analysis, the propagation of the generalized Twiss parameters in the Snake lattice allows for a better understanding of the "local coupling" concept (a term used

2023 JINST 18 P10012

in many references). To that end, the propagation of the parameter u throughout the lattice can be analyzed. Figure 8a shows that u is initially zero because we impose uncoupled initial conditions. It remains zero in all the elements that do not introduce coupling until reaching the first solenoid. We observe that if an element does not introduce coupling, the parameter u remains constant. From an eigenvector point of view, it means that the ratio between the x and y components of the eigenvector remains constant [27] because the element does not introduce more coupling than the initial coupling at the element entry. In the snake beamline, the only elements that change the parameter u are the solenoids, with their longitudinal field that couples the transverse motion. In parallel with the parameter u, we can analyze the principal and non-principal β-functions of the MR parametrization, shown in figure 9. When u is greater than 0.5, the non-principal functions become more important than the principal ones. If u remains greater than 0.5 at a solenoid output, which is the case at the end of the Snake line, the non-principal functions remain dominant until the end of the line. Moreover, when $u \to 1$, the principal functions cancel each other out. It corresponds to $\gamma \to 0$: the transfer line is then so coupled that the planes have been totally inverted (forced mode flip). A strong enough coupling is necessary to have this mode inversion along the line; nevertheless, when u tends to 1, the line is locally totally decoupled if we invert the mode identification.

When propagated in a lattice from initial conditions, the parameter u thus gives a measure of the local coupling. If initially uncoupled lattice functions are propagated into elements without local coupling, the non-principal β and α functions (or equivalently, the complex ζ functions) remain zero. Nevertheless, these parameters can be non-zero in elements without coupling if they follow lattice parts introducing coupling; the parameter u will then have a finite value that will remain constant in these elements. To support this interpretation, the parameter u can also be examined in the Spin rotator lattice, as shown in figure 10. The various observations made for the Snake lattice also hold in this example. The parameter u is constant except in the solenoids, which allow turning electron spin. We observe that the coupled insertion is designed to cancel the coupling of the solenoids. In figure 7, we can see that the non-principal functions are non-zero only in the coupled insertions; when u returns to 0, indicating a zero local coupling, the non-principal lattice functions are also zero.

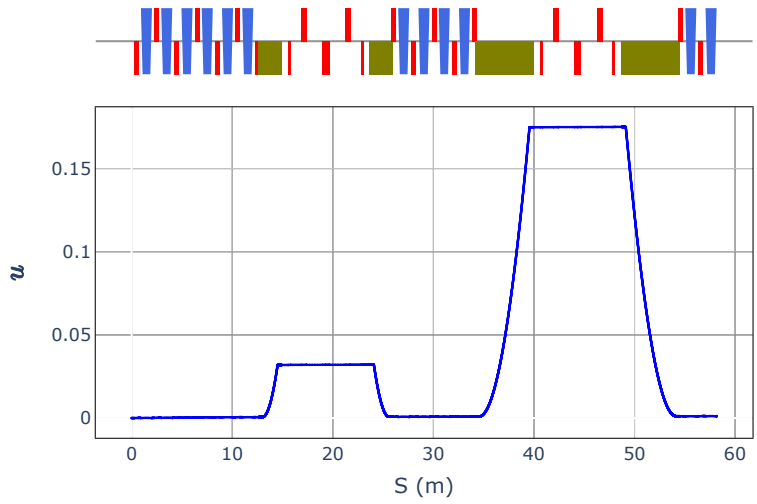

Figure 10. Parameter u of the LB parametrization, obtained by the propagation of initial lattice functions in the Spin Rotator lattice.

2023 JINST 18 P10012

The parameter u of LB, calculated with periodic conditions or by the propagation of initial lattice functions, thus gives an idea, respectively, of the lattice average coupling strength or the local coupling at a specific place in the lattice. Moreover, we have highlighted the link between this parameter and the ellipses in the physical coupled phase space. Although this parameter can be used qualitatively, it cannot be rigorously used in all cases to evaluate the coupling strength because it includes different terms that can cancel each other out in some situations, in particular when a longitudinal field is present ($R_{1,2} \neq 0$, see eq. (3.6)). The interpretation of the constant value of u in the elements not introducing coupling remains nevertheless valid because the relative importance of the x and y components of the coupled transfer matrix eigenvectors does not change if the element does not introduce any additional coupling.

5 Summary and conclusions

Transverse betatron motion coupling is a frequent occurrence, whether originating from residual coupling that appears due to imperfections or being coupling "by design" from strong systematic coupling fields. Vertical excursion FFAs exhibit strong coupling due to their longitudinal and skew quadrupolar field components. The in-depth study of their linear optics must be studied using models adapted to strongly coupled optics. To support that effort, the available parametrization methods have been briefly reviewed and applied to strongly coupled lattices to highlight the interpretation of their key parameters. The ET parametrization allows readily finding the linear invariants of motion by exploring the motion in the decoupled axes. However, the generalized lattice functions of this parametrization are not easily interpretable in terms of beam Σ-matrix. The MR parametrization allows having a lattice function interpretation similar to that of the Courant-Snyder theory, allowing to link these lattice functions to measurable beam parameters. The ET and MR parametrizations are complementary and are used for different purposes. To benchmark the different parametrization methods, these methods have been implemented in a Python interface to the Zgoubi ray-tracing code. The validation of these implementations was carried out on different example lattices with a remarkable agreement with MAD-X and PTC.

The ET parametrization, with its generalized Twiss parameters and decoupling matrix, is used to find linear invariants and to analyze the motion in linearly decoupled phase spaces, for example for the computation of the dynamic aperture. The ET parametrization was implemented in Zgoubidoo by using the method presented by Parzen in ref. [22], which can easily be generalized in higher-dimensional phase space. We obtained an excellent agreement between our results and those obtained with MAD-X, which implements the method presented by Edwards and Teng in ref. [19] and extended by Sagan and Rubin in ref. [21]. In parallel with the decoupled motion study, one can also use a parametrization of the MR category to link it with measurable quantities, such as the beam sizes. We have highlighted that the parametrizations of the MR category describe the quasi-harmonic motions in the coupled phase spaces, resulting from the eigen oscillations in the decoupled space. Depending on the chosen parametrization, one can describe the principal and non-principal oscillations either independently with parameter sets for each oscillation (WR) or with parameters describing the non-principal oscillations relative to the principal ones. The amplitudes and phase shifts are then either given explicitly (LB) or with phasors gathering amplitude and phase in the same quantity (Wolski). If the motion is studied using geometric coordinates, the phase space is

2023 JINST 18 P10012

described by the WR parameters. If the motion is expressed in canonical coordinates, the phase space is described by parameters accounting for the longitudinal field coupling, such as the LB parameters.

For studies of strongly coupled accelerators, the LB parametrization is encouraged as it provides relevant additional parameters compared to the WR description. The parameter u qualitatively evaluates the local coupling strength. It characterizes the size of the two ellipses coming from an oscillation eigenmode in the two transverse phase spaces, can be related to the local coupling concept, and can indicate a forced mode flip because it is linked to the γ parameter of the ET parametrization. The in-depth interpretation, implementation, and validation of the available parametrization methods pave the way for complete and detailed studies of the beam dynamics in strongly coupled vFFA lattices.

Acknowledgments

The authors would like to thank J-B. Lagrange for the fruitful discussions and comments on the manuscript. Marion Vanwelde is a Research Fellow of the Fonds de la Recherche Scientifique — FNRS. This work was supported at Jefferson Lab by U.S. Department of Energy under DE-AC05-06OR23177.

A Magnetic field components of a vFFA lattice

vFFAs satisfy the following scaling condition:

$$B = B_0 e^{k(Y-Y_0)}, \tag{A.1}$$

where $k = (1/B)(\partial B/\partial Y)$ is the normalized field gradient, Y_0 is the reference vertical position and B_0 is the magnetic field strength at the reference position. Assuming $Y_0 = 0$, the three magnetic field components can be written with an out-of-plane expansion of order n [11]:

$$B_X(X,Y,Z) = B_0 e^{kY} \sum_{i=0}^{n} b_{Xi}(Z) X^i, \tag{A.2}$$

$$B_Y(X,Y,Z) = B_0 e^{kY} \sum_{i=0}^{n} b_{Yi}(Z) X^i, \tag{A.3}$$

$$B_Z(X,Y,Z) = B_0 e^{kY} \sum_{i=0}^{n} b_{Zi}(Z) X^i, \tag{A.4}$$

where, by taking into account the fringe field function $g(Z)$, the coefficients of these equations are given by the following recurrence relations [11]:

$$\begin{aligned} &b_{X0}(Z) = 0, \quad b_{X,i+1}(Z) = -\frac{1}{i+1}\left(k b_{Yi} + \frac{db_{Zi}}{dZ}\right), \\ &b_{Y0}(Z) = g(Z), \quad b_{Y,i+2}(Z) = \frac{k}{i+2} b_{X,i+1}, \\ &b_{Z0}(Z) = \frac{1}{k}\frac{dg}{dZ}, \quad b_{Z,i+2}(Z) = \frac{1}{i+2}\frac{db_{X,i+1}}{dZ}. \end{aligned} \tag{A.5}$$

If we look at the field in the element body, by neglecting the fringe field ($g(Z) = const.$, $g'(Z) = 0$, $B_Z = 0$), the transverse field components can be expressed as multipolar expansions by

2023 JINST 18 P10012

rewriting the exponential in terms of its Taylor series. It is readily seen that the first-order terms of this expansion correspond to skew quadrupolar components:

$$\begin{aligned} B_X(X,Y,Z) &\simeq -B_0(kX + \frac{k^2}{2!}(2XY) + O(X^3)) \\ &\simeq -B_0 kX, \end{aligned} \tag{A.6}$$

$$\begin{aligned} B_Y(X,Y,Z) &= B_0(1 + kY + \frac{k^2}{2!}(Y^2 - X^2) + O(X^3)) \\ &\sim B_0 + B_0 kY. \end{aligned} \tag{A.7}$$

References

[1] E.D. Courant and H.S. Snyder, *Theory of the alternating gradient synchrotron*, *Ann. Phys.* **3** (1958) 1.

[2] M. Hofer and R. Tomás, *Effect of local linear coupling on linear and nonlinear observables in circular accelerators*, *Phys. Rev. Accel. Beams* **23** (2020) 094001.

[3] R. Talman, *The Mobius accelerator*, *Phys. Rev. Lett.* **74** (1995) 1590.

[4] A. Burov, *Circular Modes for Flat Beams in the LHC*, *Phys. Rev. ST Accel. Beams* **16** (2013) 061002 [arXiv:1301.7743].

[5] C. Du, J. Wang, D. Ji and S. Tian, *Studies of round beam at HEPS storage ring by driving linear difference coupling resonance*, *Nucl. Instrum. Meth. A* **976** (2020) 164264.

[6] Y.M. Shatunov et al., *Project of a new electron positron collider VEPP-2000*, *Conf. Proc. C* **0006262** (2000) 439.

[7] T. Ohkawa, *FFAG electron cyclotron*, *Bull. APS* **30** (1955) 20.

[8] G. Leleux, J. Proy and M. Salvat, *F.F.A.G. Helicoïdal etude de la stabilite betatron*, Tech. Rep. Rapport OC 70, Service de Physique Appliquée, section d'Optique Corpusculaire (1959).

[9] J. Teichmann, *Accelerators with vertically increasing field*, *Sov. J. At. Energ.* **12** (1963) 507.

[10] S. Brooks, *Vertical orbit excursion fixed field alternating gradient accelerators*, *Phys. Rev. ST Accel. Beams* **16** (2013) 084001.

[11] S. Machida, D.J. Kelliher, J.-B. Lagrange and C.T. Rogers, *Optics Design of Vertical Excursion Fixed-Field Alternating Gradient Accelerators*, *Phys. Rev. Accel. Beams* **24** (2021) 021601 [arXiv:2011.10783].

[12] M. Vanwelde et al., *Modeling and implementation of vertical excursion FFA in the Zgoubi ray-tracing code*, *Nucl. Instrum. Meth. A* **1047** (2023) 167829.

[13] T. Ohkawa, reported at the *Annual meeting of JPS*, 1953.

[14] K.R. Symon et al., *Fixed-field alternating-gradient particle accelerators*, *Phys. Rev.* **103** (1956) 1837.

[15] A.A. Kolomensky and A.N. Lebedev, *Theory of cyclic accelerators*, North-Holland, Amsterdam (1966).

[16] D. Newsham, R.P. Johnson, R. Sah, S.A. Bogacz, Y.-C. Chao and Y. Derbenev, *Simulations of parametric-resonance ionization cooling*, in the proceedings of the *22nd Particle Accelerator Conference*, Albuquerque, NM, U.S.A., 25–29 June 2007, pp. 2927–2929.

[17] S.A. Bogacz and G.A. Krafft, *Accelerator Physics*, in *U.S. Particle Accelerator School*, Fort Collins, CO, U.S.A., 10–21 June 2013.

2023 JINST 18 P10012

[18] H.K. Sayed, *Compensation Techniques in Accelerator Physics*, Ph.D. thesis, JLAB-ACP-11-1526, DOE/OR/23177-2396, 1057574, Thomas Jefferson National Accelerator Facility, Newport News, VA, U.S.A. (2011).

[19] D.A. Edwards and L.C. Teng, *Parametrization of linear coupled motion in periodic systems.*, *IEEE Trans. Nucl. Sci.* **20** (1973) 885.

[20] I. Borchardt, E. Karantzoulis, H. Mais and G. Ripken, *Calculation of Beam Envelopes in Storage Rings and Transport Systems in the Presence of Transverse Space Charge Effects and Coupling*, *Z. Phys. C* **39** (1988) 339.

[21] D. Sagan and D. Rubin, *Linear analysis of coupled lattices*, *Phys. Rev. ST Accel. Beams* **2** (1999) 074001.

[22] G. Parzen, *The Linear parameters and the decoupling matrix for linearly coupled motion in six-dimensional phase space*, acc-phys/9510006.

[23] Y. Luo, *Linear coupling parametrization in the action-angle frame*, *Phys. Rev. ST Accel. Beams* **7** (2004) 124001 [*Erratum ibid.* **9** (2006) 039901].

[24] A. Wolski, *Alternative approach to general coupled linear optics*, *Phys. Rev. ST Accel. Beams* **9** (2006) 024001.

[25] A. Wolski, *A simple way to characterize linear coupling in a storage ring*, Tech. Rep. LBNL-54774, 822969, LBNL, Berkeley, CA, U.S.A. (2004).

[26] A. Wolski and M. Woodley, *Normal form analysis of linear beam dynamics in a coupled storage ring*, in the proceedings of the 9^{th} *European Particle Accelerator Conference (EPAC 2004)*, Lucerne, Switzerland, 5–9 July 2004, pp. 1503–1505.

[27] V.A. Lebedev and S.A. Bogacz, *Betatron Motion with Coupling of Horizontal and Vertical Degrees of Freedom*, 2010 *JINST* **5** P10010 [arXiv:1207.5526].

[28] C. Hernalsteens, R. Tesse and M. Vanwelde, *Zgoubidoo*, https://ulb-metronu.github.io/zgoubidoo/, 2022.

[29] F. Méot, *The ray-tracing code Zgoubi – Status*, *Nucl. Instrum. Meth. A* **767** (2014) 112.

[30] *Methodical Accelerator Design (MAD-X)*, https://mad.web.cern.ch.

[31] F. Schmidt, E. Forest and E. McIntosh, *Introduction to the polymorphic tracking code: Fibre bundles, polymorphic Taylor types and "Exact tracking"*, Tech. Rep. CERN-SL-2002-044-AP, KEK-REPORT-2002-3, CERN, Geneva (2002).

[32] L.C. Teng, *Concerning n-Dimensional Coupled Motions*, Tech. Rep. FERMILAB-FN-0229, FERMILAB, Batavia, IL, U.S.A. (1971).

[33] L. Deniau et al., *Development of the cern accelerator code mad-x for present and future large colliders*, unpublished, 2020.

[34] P.P. Bagley and D.L. Rubin, *Correction of transverse coupling in a storage ring*, in the proceedings of the *IEEE Particle Accelerator Conference*, Chicago, IL, U.S.A., 20–23 March 1989, pp. 874–876 [DOI:10.1109/pac.1989.73286].

[35] Y. Luo et al., *Continuous measurement of global difference coupling using a phase-locked-loop tune meter in the Relativistic Heavy Ion Collider*, *Phys. Rev. ST Accel. Beams* **9** (2006) 124001.

[36] F. Desforges, *Implementation of a coupled treatment of the one-turn mapping in the ray-tracing code Zgoubi*, Tech. rep. C-AD Note C-A/AP/461, BNL-98559-2012-I, BNL, Upton, NY, U.S.A. (2012).

2023 JINST 18 P10012

[37] F. Willeke and G. Ripken, *Methods of Beam Optics*, *AIP Conf. Proc.* **184** (2008) 758.

[38] H. Wiedemann, *Particle accelerator physics*, fourth edition, Springer (2015).

[39] F. Méot, *The Ray tracing code Zgoubi*, *Nucl. Instrum. Meth. A* **427** (1999) 353.

[40] F. Méot and J.S. Berg, *Zgoubi*, http://sourceforge.net/projects/zgoubi/.

[41] F. Méot, *6-D beam dynamics simulations in FFAGs using the ray-tracing code Zgoubi*, *ICFA Beam Dyn. Newslett.* **43** (2007) 44.

[42] F. Lemuet and F. Méot, *Developments in the ray-tracing code Zgoubi for 6-D multiturn tracking in FFAG rings*, *Nucl. Instrum. Meth. A* **547** (2005) 638.

[43] J. Fourrier, F. Martinache, F. Meot and J. Pasternak, *Spiral FFAG lattice design tools. Application to 6-D tracking in a proton-therapy class lattice*, *Nucl. Instrum. Meth. A* **589** (2008) 133.

[44] M. Vanwelde et al., *The Zgoubidoo python framework for ray-tracing simulations with Zgoubi: applications to fixed-field accelerators*, *J. Phys. Conf. Ser.* **2420** (2023) 012039.

2023 JINST 18 P10012